Fig. 6. Evaluation of three different combinations of (T_i, k_p), corresponding to symbols ▲, ● and ■ on Fig 5, applied on a single virtual sheep, showing the instantaneous RR response (A) and the VNS current obtained as output of the PI controller (B).

the contrary, the values inside Γ yield a satisfying compromise between accuracy and time response.

B. Experimental Validation

The controller was tested on six sheep, three of them anesthetized by two different anesthetics (Etomidate and Isoflurane). In order to validate the ranges of T_i and k_p derived from the previous MBD, and since the animal experimentation time is limited, two approaches with a reduced set of combinations of T_i and k_p were studied. For the first sheep, k_p was fixed to $k_p = 0.005 \in \Gamma$ and several values of T_i are explored. The target value was set at 110% of the baseline RR, measured at the beginning of the experimentation, so as to observe the convergence response for large T_i values $(T_i > 1)$. For all other sheep, different values of k_p are used, while fixing $T_i = 0.4 \in \Gamma$. RR target values were set at 105% and 110% of the baseline RR, but only results leading to attainable target values (without premature ventricular contractions) were kept. Due to technical reasons (recording problems), performance measures for sheep 5 at 105% were not computed.

1) Experimental Validation of T_i: The sheep was anesthetized by Isoflurane. The target RR is set at 110% of the RR baseline and five values of T_i were tested. Fig. 7 shows that an increase of T_i is associated with reduced oscillations but also with a reduced speed of convergence. These results are in concordance with the sensitivity analysis presented in Fig. 5. Note that the combination $(T_i = 0.4, k_p = 0.005) \in \Gamma$ yields the best compromise between precision and speed of convergence. Results given in Table I (see Sheep 1) confirm these conclusions.

2) Experimental Validation of k_p: Sheep 2 was anesthetized by Etomidate. Results are presented for a target RR set at 105% of the RR baseline, with T_i fixed at 0.4, and five values of k_p. Fig. 8 shows that, in all cases, the target is reached. As expected, when k_p is increased, the speed of convergence is increased, but MSE and %OS are increased too (see Table I, Sheep 2). It
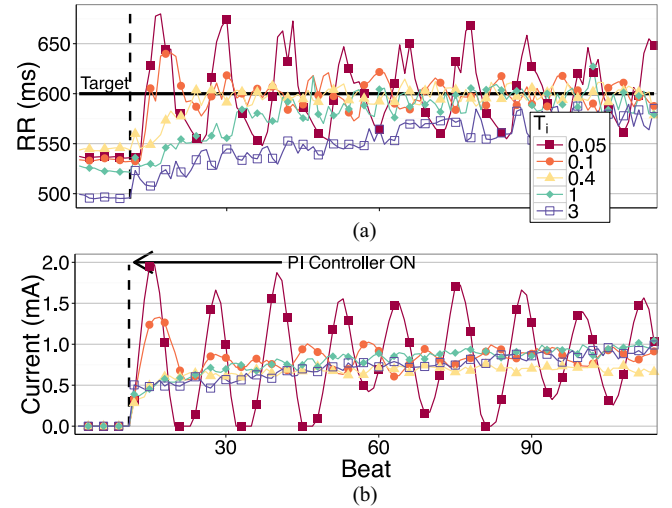

Fig. 7. Experimental results on sheep 1 anesthetized by Isoflurane with a target set at 110% of the RR baseline. Five values of T_i were tested, while observing the instantaneous RR interval of the sheep (A) and the VNS current obtained from the controller (B).

TABLE I
PERFORMANCE MEASURES ON ANIMAL EXPERIMENTATION; A = ANESTHETICS, I = ISOFLURANE, E = ETOMIDATE

Sheep	A	Target	k_p	T_i	MSE	%OS	T_r	Baseline RR (mean±std)
1	I	110%	0.005	0.05	909.32	125.60	4	537.90 ± 1.09
				0.1	108.31	61.32	5	534.10 ± 1.50
				0.4	53.97	26.24	14	544.16 ± 1.36
				1	149.73	23.83	31	525.35 ± 1.52
				3	1000.45	0	–	499.17 ± 2.00
2	E	105%	0.012	0.4	246.10	152.87	1	653.70 ± 0.76
			0.008		99.32	95.67	3	659.57 ± 0.83
			0.005		51.92	81.08	7	665.01 ± 0.95
			0.001		13.35	11.53	51	663.68 ± 1.01
			0.0001		1.01	0	81	652.03 ± 0.53
3	E	105%	0.005	0.4	198.67	145.20	12	426.25 ± 0.97
			0.001		42.90	50.39	63	420.96 ± 1.27
	I	105%	0.005		392.97	144.49	1	549.68 ± 0.98
			0.001		157.53	56.35	67	549.64 ± 1.01
4	E	105%	0.01	0.4	56.68	35.51	17	672.17 ± 4.72
			0.005		88.58	23.15	39	672.71 ± 5.36
5	E	105%	0.005	0.4	75.46	101.39	19	400.03 ± 1.14
			0.001		33.36	90.12	91	399.91 ± 1.12
		110%	0.005		780.10	133.01	8	400.10 ± 1.15
			0.001		133.60	6.02	56	400.44 ± 1.02
	I	110%	0.005		838.60	92.61	9	578.52 ± 1.23
			0.001		116.60	5.96	48	581.23 ± 2.08
6	E	105%	0.005	0.4	685.49	26.37	7	595.30 ± 1.01
			0.001		56.28	7.54	26	598.12 ± 1.17
		110%	0.005		61.18	7.91	7	597.53 ± 0.94
			0.001		21.03	4.63	44	598.30 ± 0.83
	I	105%	0.005		105.16	10.35	8	693.41 ± 0.68
			0.001		124.80	8.85	40	687.57 ± 0.92
		110%	0.005		25.92	5.02	14	694.87 ± 1.23
			0.001		23.04	4.75	54	691.40 ± 1.16

is interesting to note that, among the tested values, the value $k_p = 0.005 \in \Gamma$, yields the best compromise between speed of convergence (T_r) and accuracy (MSE and %OS).

3) Global Experimental Results: Table I, presents the experimental results on all the sheep included in our experimental
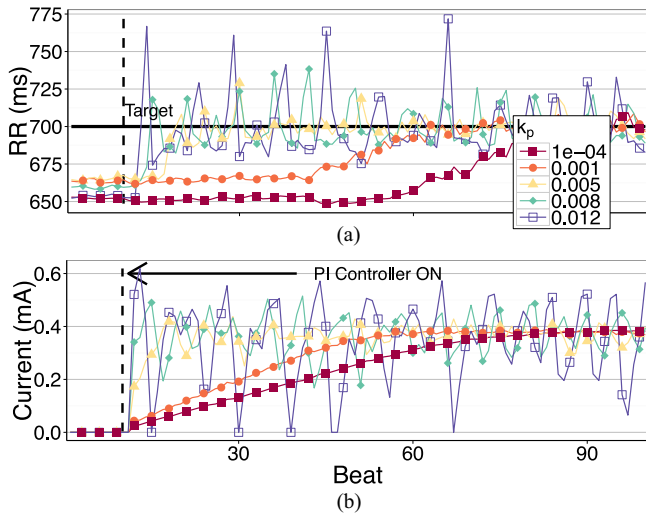
Fig. 8. Experimental results on sheep 2, anesthetized by Etomidate with a target set at 105% of the RR baseline. Five values of k_p were tested, while observing the instantaneous RR interval of the sheep (A) and the VNS current obtained from the controller (B).

evaluation, using different targets and control parameter values. Note that the use of k_p values higher than 0.012 (i.e., the maximum value of k_p analyzed on the virtual population) was avoided during the experimentation, after sheep 2, in order to ensure a safety condition. In all cases, the expected performance is achieved using PI parameters that are inside the domain Γ, derived from the MBD approach. Table I also presents the baseline values of RR interval. No correlation was found between baseline RR values and the obtained performance indicators, showing the controller's ability to adapt to various conditions.

VI. DISCUSSION

Previous studies have shown the utility of using a theoretical approach in order to improve the design of medical devices. For instance, in [28], a first-order transfer function is used to represent the relationship between the current delivered to a neuron (input of the controlled system) and the interspike intervals of the neuron (output of the controlled system). In [3], the relationship between the VNS frequency (input of the controlled system) and the RR interval (output of the controlled system) is modeled by a first-order transfer function. The PI controllers designed in both papers work successfully in a limited range. However, the authors suggest that better results may be reached by using more detailed models, which can take into account the more complex (and often nonlinear) function of the underlying system. As a difference to these previous studies, the MBD presented in our paper is based on an integrated physiological model including nonlinear dynamics and relies on a complete sensitivity analysis of this model. Therefore, the designed PI controller may perform better in a larger range, since nonlinearities and physiological delays are taken into account. Moreover, a safer behavior is ensured because the controller was tested on a large virtual population, obtained from significant variations of the model parameter values, and leading to a large variety of responses to VNS. To our knowledge, this paper is the first to describe such a model-based approach, based on an

integrated model and including the creation of a virtual population associated with an exhaustive sensitivity analysis of control parameters.

Concerning the particular application developed in this paper for closed-loop VNS therapy, the difficulty is to find an optimal set of PI parameters presenting the best compromise between time of convergence and accuracy, while assuring safe stimulation conditions and smooth transitions on the current applied to the nerve. For instance, we can observe in Figs. 7 and 8(B) that the applied current during VNS tends to 1 and 0.4 mA, respectively. However, the dynamics of the VNS current depend directly on the control parameters (Figs. 7 and 8(B)). Low (k_p) and high (T_i) are associated with slow, low-amplitude dynamics of the VNS current, while high (k_p) and low (T_i) provoke rapid, high-amplitude changes on the applied current, and oscillations in the observed RR interval. The set of control parameter values, identified through the sensitivity analysis phase within the Γ domain, lead to an appropriate adjustment on VNS current dynamics in the experimental evaluation, provoking suitable changes on the observed RR interval, and a good compromise between accuracy and speed of convergence. Moreover, the proposed PI controller provides satisfactory results for both anesthetic agents, Isoflurane and Etomidate (see I and E in Table I, respectively), that are associated with two different autonomic states. This finding is particularly interesting for the use of the proposed controller in clinical practice, since the autonomic states of a patient could be affected by several long and short-term influences. Furthermore, since most of the control parameter values used during experimental evaluation were kept within the Γ domain, the evaluated PI controllers could ensure a safe and optimized response for a majority of circumstances.

Limitations of this study are mainly related to the experimentation phase. Although the experimental conditions were standardized (anesthesia, regulated breath,...), the uncontrolled variations of environmental conditions (evolution of the anesthetic's effect during the experimentation, physiological variations, ...) made the RR baseline value evolves through time, even for the same sheep under the same anesthetic agent (Table I, last column). This effect, which can be clearly seen in Fig. 7(A), provokes a slight drift on the optimal required current for attaining the target RR, which was defined with respect to the initial RR baseline value. However, this RR baseline variability does not affect the control strategy, since the target RR was reached in all cases, and no correlation was found between RR baseline values and the obtained PI performance. Another limitation of this study is related to the model. Although the proposed model is more detailed than those used in previous related studies, it may be improved by a better representation of the electrode–nerve interface. Current studies of our team are directed to a better characterization of the autonomic response for different VNS parameters [29].

VII. CONCLUSION

In this paper, we proposed a model-based framework for the design of control modules for medical devices. This framework allowed us to design PI controllers which work synchronously

with the heart period, for regulating the heart rate by modifying the stimulation current applied to the VN.

A physiological model representing the CVS of a sheep, including the cardiac response to VNS was used to generate a virtual population. Sensitivity analyses were performed by varying parameters of the control system and the physiological model in order to estimate a domain of interest in the space of the control parameters. The PI controller derived from the proposed MBD approach was experimentally validated on six sheep, by using two different anesthetics. Results clearly show the interest of using a model-based approach in order to determine the parameter values of a PI controller and to optimize the dynamic performance of the closed-loop regulator.

The proposed MBD framework can be generalized to other applications. Our current study is directed to the integration and evaluation of other control methods for the same VNS application (same model of the plant, but different controller), but also to the application of PID-type controllers for the optimization of cardiac resynchronization therapy (same controller, but different plant model). This MBD approach may also help to minimize animal experimentation for the design of closed-loop medical devices.

REFERENCES

[1] R. H. Howland, "Vagus nerve stimulation," *Curr. Behav. Neurosci. Rep.*, vol. 1, no. 2, pp. 64–73, 2014.

[2] C. Wu. (2013, Dec.). "Closed-loop stimulation: An investigational treatment for refractory epilepsy," *Int. Neuromod. Soc.*, [Online]. Available: http://www.neuromodulation.com/assets/documents/Fact_Sheets/fact_sheet_epilepsy_loop.pdf

[3] M. Tosato *et al.*, "Closed-loop control of the heart rate by electrical stimulation of the vagus nerve," *Med. Bio. Eng. Comput.*, vol. 44, no. 3, pp. 161–169, 2006.

[4] H. P. Buschman *et al.*, "Heart rate control via vagus nerve stimulation," *Neuromodulation*, vol. 9, no. 3, pp. 214–220, 2006.

[5] Y. Zhou *et al.*, "An implanted closed-loop chip system for heart rate control: System design and effects in conscious rats," *J. Biomed. Res.*, vol. 24, no. 2, pp. 107–114, 2010.

[6] H. M. R. Ugalde *et al.*, "On-off closed-loop control of vagus nerve stimulation for the adaptation of heart rate," in *Proc. IEEE Eng. Med. Biol. Soc. Int. Conf.*, Aug. 2014, pp. 6262–6265.

[7] M. S. Waninger *et al.*, "Electrophysiological control of ventricular rate during atrial fibrillation," *Pacing Clin. Electro*, vol. 23, no. 8, pp. 1239–1244, 2000.

[8] Y. Zhang *et al.*, "Optimal ventricular rate slowing during atrial fibrillation by feedback av nodal-selective vagal stimulation," *Amer. J. Physiol. Heart Circ. Physiol.*, vol. 282, no. 3, pp. H1102–H1110, 2002.

[9] H. Chen and B. Gao, *Nonlinear Estimation and Control of Automotive Drivetrains*. New York, NY, USA: Springer-Verlag, 2013.

[10] D. Cieslar *et al.*, "Model based approach to closed loop control of 1-D engine simulation models," *Control Eng. Pract.*, vol. 29, pp. 212–224, 2014.

[11] G. D. Kontes *et al.*, "Intelligent BEMS design using detailed thermal simulation models and surrogate-based stochastic optimization," *J. Process Control*, vol. 24, no. 6, pp. 846–855, 2014.

[12] D. Faille *et al.*, "Control design model for a solar tower plant," *Energy Procedia*, vol. 49, pp. 2080–2089, 2014.

[13] D. Riu *et al.*, "Control and design of dc grids for robust integration of electrical devices. Application to aircraft power systems," *Int. J. Electr. Power Amp; Energy Syst.*, vol. 58, pp. 181–189, 2014.

[14] K. T. V. Koon *et al.*, "Atrioventricular delay optimization in cardiac resynchronization therapy assessed by a computer model," in *Proc. IEEE Comput. Cardiol.*, 2010, pp. 333–336.

[15] A. I. Hernández *et al.*, "Model-based interpretation of cardiac beats by evolutionary algorithms: Signal and model interaction," *Artif. Intell. Med.*, vol. 26, no. 3, pp. 211–235, 2002.

[16] D. Ojeda *et al.*, "Towards an atrio-ventricular delay optimization assessed by a computer model for cardiac resynchronization therapy," presented at the SPIE 8922 IX Int. Seminar Medical Information Processing Analysis, Mexico city, Mexico, 2013.

[17] D. Ojeda *et al.*, "Sensitivity analysis and parameter estimation of a coronary circulation model for triple-vessel disease," *IEEE Trans. Biomed. Eng.*, vol. 61, no. 4, pp. 1208–1219, Apr. 2014.

[18] D. Ojeda *et al.*, "Analysis of a baroreflex model for the study of the chronotropic response to vagal nerve stimulation," in *Proc. IEEE/EMBS 7th Int. Neural Eng. Conf.*, Apr. 2015, pp. 541–544.

[19] B. Smith *et al.*, "Simulation of cardiovascular system diseases by including the autonomic nervous system into a minimal model," *Comput. Methods Programs Biomed.*, vol. 86, no. 2, pp. 153–160, 2007.

[20] V. L. Rolle *et al.*, "Embedding a cardiac pulsatile model into an integrated model of the cardiovascular regulation for heart failure follow-up," *IEEE Trans. Biomed. Eng.*, vol. 58, no. 10, pp. 2982–2986, Oct. 2011.

[21] A. I. Hernández *et al.*, "Integration of detailed modules in a core model of body fluid homeostasis and blood pressure regulation," *Progress Biophys. Molecular Biol.*, vol. 107, no. 1, pp. 169–182, 2011.

[22] M. Ursino and E. Magosso, "Acute cardiovascular response to isocapnic hypoxia. i. a mathematical model," *Amer. J. Physiol. Heart Circul. Physiol.*, vol. 279, no. 1, pp. H149–H165, 2000.

[23] W. Gersch and E. Dong, "A note on Warner's vagus heart rate control model," *IEEE Trans. Biomed. Eng.*, vol. BME-20, no. 2, pp. 145–148, Mar. 1973.

[24] J. C. Helton *et al.*, "A comparison of uncertainty and sensitivity analysis results obtained with random and latin hypercube sampling," *Reliab. Eng. Syst. Safety*, vol. 89, no. 3, pp. 305–330, 2005.

[25] R. Iman and W. Conover, "Small sample sensitivity analysis techniques for computer models, with an application to risk assessment," *Commun. Stat. Theory Meth.*, vol. A9, no. 17, pp. 1749–1842, 1980.

[26] H. M. R. Ugalde *et al.*, "Model-based design of control modules for neuromodulation devices," in *Proc. IEEE/EMBS 7th Int. Neural Eng. Conf.*, Apr. 2015, pp. 462–465.

[27] D. Andreu *et al.*, "A distributed architecture for activating the peripheral nervous system," *J. Neural Eng.*, vol. 6, no. 2, p. 026001, 2009.

[28] O. Miranda-Domínguez *et al.*, "Firing rate control of a neuron using a linear proportional-integral controller," *J. Neural Eng.*, vol. 7, no. 6, p. 066004, 2010.

[29] L. Rousselet *et al.*, "Influence of vagus nerve stimulation parameters on chronotropism and inotropism in heart failure," in *Proc. IEEE Int. 36th Annu. Eng. Med. Biol. Soc.*, Aug. 2014, pp. 526–529.